Advances in Geosciences Konstantinos Perakis & Athanasios Moysiadis, Editors
EARSeL, 2012

Mosaic Methods for Improving the Accuracy of Interferometric Based Digital Elevation Models

Chris Choussiafis[1],Vassilia Karathanassi[1] and Konstantinos Nikolakopoulos[2]
[1]*National and Technical University of Athens, School of Rural and Surveying Engineering, Laboratory of Remote Sensing, Athens, Greece;*
xristos.xousiafis@gmail.com; karathan@survey.ntua.gr
[2]*Institute of Geology and Mineral Exploration, Athens, Greece;*
knikolakopoulos@igme.gr

Abstract. The last two decades, SAR interferometry is used in order to produce Digital Elevation Model (DEM) for wide areas. However, the DEM produced by only one interferometric pair is characterized by low accuracy, due to several parameters that affect the final result. In this study, the improvement of the DEM accuracy is attempted through the production of a mosaic DEM derived by multiple interferometric-based DEMs. Two methods are used to create the mosaic DEM. According to the first method, the entire height information included in the various interferometric-based DEMs is introduced in the procedure. In the second method only the selected areas of the interferometric-based DEMs participate in the production of the mosaic DEM. The selection is based on the comparison between interferometric-based DEMs with another ancillary DEM (e.g. ASTER GDEM). For both methods, the mosaic DEM generation is based on the precision file which provides a height accuracy map that is estimated from parameters such as coherence, baseline and wavelength. Although this file is not always reliable it can be used to define weights for the height values of the available interferometric-based DEMs during the mosaic DEM generation. The Root Mean Square Error (RMSE) is used to estimate the vertical accuracy. The validation of the DEMs is achieved by comparing them with a sufficient number of ground control points as well with an accurate reference DEM. The mosaic DEM produced by the first method does not yield improvements in accuracy, whereas the second method provides significant improvements depending on the accuracy of the reference DEM being used.

Keywords. InSAR, DEM, interferometry, coherence, ALOS PALSAR, fusion.

1. Introduction

SAR interferometry (InSAR) is the remote sensing technique which exploits the phase difference of two SAR acquisitions in order to produce accurate Digital Elevation Model (DEM) [1], [2], [3]. InSAR is one of the three main techniques for the DEM production of wide areas. The two other techniques are the airborne laser scanning and the automatic optical image matching which is the direct successor of manual stereo photogrammetric measurements [4], [5]. Each of these techniques has its own strengths and weaknesses. Aiming at the improvement of the quality and accuracy of a DEM, several efforts towards the direction of fusion of overlapping DEMs have been made. The DEM resulting from fusion methods should be geometrically accurate by depicting the correct height information of the area, clean by eliminating blunders and errors which are present in the initial data and complete by modelling all the area in the highest possible resolution [6], [7]. The multi-source DEMs usually have different characteristics, such as pixel size, height accuracy, etc., and are generated from data of different acquisition techniques and/or dates. For multi-source DEMs combination, a number of DEM fusion strategies have been proposed [8], [9], [10], [11], [12], [13]. Among them, some strategies address the problem of fusion of DEMs produced by interferometric processing [14], [15].

According to Gens and Van Genderen [16], there are several parameters that affect the final result of the interferometric process. The accuracy of the DEM achieved using only one interferometric pair is usually very low. In order to produce an accurate mosaic DEM, the fusion of multiple interferometric-based DEMs is applied. The fusion is based on a weighted averaging. The success of the fusion depends on the local quality of each DEM. The quality is represented on the height accuracy map or otherwise on the height error map of each individual interferometric - based DEM. For each pixel, the height accuracy map contains an estimation of the accuracy that is used as local weight during the averaging process.

This paper investigates the production of a mosaic DEM surface through the fusion of interferometric-based DEMs, and the use of a weighted averaging. Two methods have been used to create the mosaic DEM. According to the first method, the entire height information included in the various interferometric-based DEMs is introduced in the procedure. In the second method, only selected areas of the interferometric-based DEMs participate in the production of the mosaic DEM. In both methods, the DEMs were in grid format, and the mosaic DEM was generated, based on the height accuracy maps provided by the SARscape software. The validation of interferometric-based DEMs and mosaic DEMs has been performed using two state of the art techniques. In the first, DEMs are compared with a sufficient number of ground control points, whereas in the second with an accurate reference DEM.

2. Fusion methods

The methods used for the fusion of the interferometric-based DEMs are based on height accuracy maps. When SARscape software [17] is used, the final step of the process that is applied on an interferometric (pair) includes phase to height conversion and geocoding. Among the associated outputs, the height accuracy map file exists. In this file, for each grid point of the produced DEM, the accuracy of calculations for the height estimation is stored. The height accuracy map has the same dimensions with the produced DEM and can be used as an input to the proposed fusion methods. Values in the accuracy map are derived according to the formula:

$$\sigma = \sqrt{\frac{1-\gamma^2}{2\gamma^2}}\frac{\lambda R \sin\theta}{4\pi B_n} \quad (1)$$

where for each pixel, σ is the value of accuracy, γ the interferometric coherence value, R is the slant range distance and θ is the local incidence angle, λ is the wavelength and B_n is the normal baseline component.

The first fusion method (1st_Method) for the production of the mosaic DEM is the one proposed by SARscape and it is based on the fusion of the entire height information included in the various interferometric-based produced DEMs. For each pixel, the combination of the height values from different interferometric-based DEMs is based on the weighted average rule. For each pixel in the produced mosaic DEM, the height value is calculated as following:

$$H_{mDEM} = \frac{w_1 H_1 + \cdots + w_n H_n}{w_1 + \cdots + w_n} \quad (2), \quad w_i = \frac{1}{\sigma_i^2}, \; i=1,\ldots,n \quad (3)$$

where $H_1,\ldots,H_n$ are the height values in $DEM_1,\ldots,DEM_n$ respectively, and $w_1,\ldots,w_n$ are the respective weights. The weights are required for quantifying the contribution of the individual DEMs. They are based on the accuracy map values σ (formula 3).

The main advantage of this method is that the discontinuities and especially the void pixels are eliminated in the resulting mosaic DEM. The disadvantage of the method is that the resulting DEM completely depends on the height accuracy maps. In fact, the height accuracy map does not always reflect the quality of the produced DEM [5], [8], [18]. More specifically, it is noted that pixels with excellent height accuracy in the original DEMs, significantly vary from the real height in the mosaic DEM. On the contrary, there are pixels of lower height accuracy, for which the calculated height values approach the real height after mosaicing. These discrepancies appear in areas that present trivial errors in the height accuracy map, although they present blunders or significant errors in the interferometric-based DEMs.

The second fusion method (2^{nd}_Method) was developed by the authors and aims at the enhancement of the reliability of the height accuracy map. The proposed procedure is shown in Figure 1. In order to perform the enhancement and generate the mosaic DEM with improved height accuracy, it is crucial to have an ancillary DEM. The ancillary DEM could be a global DEM (e.g. Aster GDEM v2) or a local DEM produced by other methods, such as digitalization of existing topographic maps, automatic optical image matching, etc. The better the accuracy of the ancillary DEM is, the better the accuracy of the final mosaic DEM will be. The ancillary DEM contributes to the evaluation of the interferometric-based DEMs and is used for masking the areas which present not only blunders but also errors beyond a defined threshold. The same masks are also applied on every individual height accuracy map. In the final step of the procedure, the weighted average rule (formula 2 and 3) is applied.

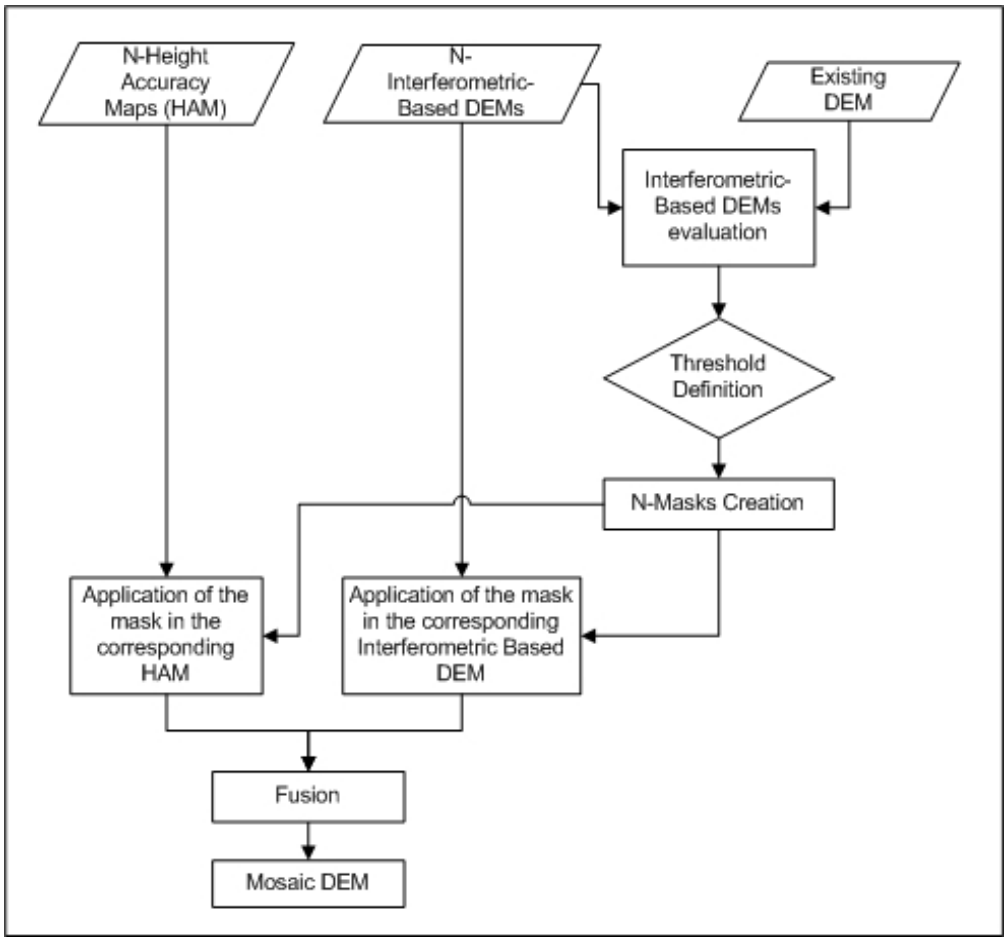

Figure 1: Flow chart of the proposed fusion methodology.

The choice of the threshold for masking the original DEMs is the key point of the proposed method. Based on several experiments with various ancillary DEMs, it was concluded that this threshold should be around the vertical accuracy of the ancillary DEM. In particular, it was observed that the value of the vertical accuracy for confidence level 95% (1.96*RMS error), when used as threshold, yields the best mosaic DEM.

3. Dataset and processing

The study area is located in the centre of Peloponissos, southern Greece and is approximately 900Km^2. It is a mountainous area with intense relief. The elevation ranges between 175m and 2015m. Over this test area 11 Single Look Complex (SLC) ALOS/PALSAR SAR (L band) acquisitions were available in FBS or FBD mode (High resolution mode, Fine Beam Single or Dual polarization). Specifically, 22 interferometric pairs were formed using as master files only the SAR acquisitions in FBS mode. The only restriction was set on the normal component of the baseline which should be less than the half critical baseline. Using as master files the ALOS/PALSAR SAR acquisitions in FBS mode, the critical baseline is approximately 13.5 Km. Therefore the selected interferometric pairs has normal component of the baseline less than 6.7 Km.

The interferometric methodology was applied on each pair using the SARscape software. Using InSAR for DEM generation, the height information for each pixel was estimated from the unwrapped phase values. According to a general model, interferometric phase can be written as:

$$\varphi = \varphi_{flat} + \varphi_{topo} + \varphi_{defo} + \varphi_{atm} + \varphi_{noise} \quad (4)$$

where φ is the interferometric phase, φ_{flat} is the flat earth phase, φ_{topo} is the topographic phase, φ_{defo} is the deformation phase, φ_{atm} is the atmospheric delay phase and φ_{noi} is the noise. In order to obtain an accurate DEM by unwrapping the phase φ, it is necessary to eliminate the components of equation (4) that do not contribute to height information. The flat earth component can be removed by using the orbit information correction, as well as an external DEM to generate the topographic phase which is then subtracted from the interferogram [19], [20]. Within this study, the external DEM used was the ASTER GDEM. The deformation component can be ignored when the time interval between the SAR acquisitions is relatively short. For ALOS/PALSAR SAR acquisitions the minimum time interval is 46 days. For simplicity reasons, ground deformations are not supposed in the study area, and interferometric pairs with time interval from 46 to 368 days are examined. As far as the atmospheric component concerns, it mainly depends on the water vapour content of the atmosphere and is considered as an error in non atmospheric applications. Finally, the noise component refers to thermal noise and the contribution of changes of individual scatterers. The noise component is removed by applying filtering techniques on the interferogram and/or SAR images. So, by removing or ignoring the components that do not contribute to height information, (4) can be written as following:

$$\varphi = \varphi_{topo} \quad (5)$$

During the interferometric process, none ground control point was used. The generated DEMs were resampled to 10m pixel spacing.

For each interferometric-based DEM, a validation was performed using a standard statistical analysis with: a) 215 existing ground control points (GCPs), and b) a reference DEM. These datasets were used in order to a) evaluate the DEM accuracy on specific points, and b) have a better assessment of the average accuracy. The reference DEM (rDEM) was provided by

KTIMATOLOGIO S.A.. This DEM has a 5m pixel size, and its average accuracy was estimated to be 2.08m according to GCPs evaluation. The main characteristics of the interferometric pairs and the RMS error for each produced DEM are shown in Table 1. It is observed that the majority of the produced interferometric-based DEMs present significant error. Only three interferometric pairs produce DEMs that present errors less than 10m when compared with the GCPs. This error is considered quite acceptable for wide area DEMs.

Table 1. Main characteristics of the interferometric pairs and RMS error of each DEM.

s/n	Master	Slave	Baseline (normal component)	Time Interval	Polarization		Height of ambiguity (2π)	RMS error	
					Master	Slave		GCPs	rDEM
1	20081110	20090210	824.14	92	HH	HH	78.40	21.64	16.52
2	20081110	20090628	1488.75	230	HH	HH/HV	43.41	26.18	22.58
3	20081110	20090813	1458.65	276	HH	HH/HV	44.63	14.53	12.90
4	20081110	20090928	1851.62	322	HH	HH/HV	34.95	37.61	35.26
5	20081226	20090210	671.24	46	HH	HH	95.93	17.33	14.70
6	20081226	20090628	1336.12	184	HH	HH/HV	48.30	45.14	38.21
7	20081226	20090813	1311.42	230	HH	HH/HV	49.35	33.84	24.72
8	20081226	20090928	1699.18	276	HH	HH/HV	38.05	37.61	35.26
9	20081226	20091229	2337.95	368	HH	HH	27.64	15.61	15.00
10	20090210	20090628	669.17	138	HH	HH/HV	96.68	15.68	23.94
11	20090210	20090813	731.59	184	HH	HH/HV	90.51	21.64	28.11
12	20090210	20090928	1035.05	230	HH	HH/HV	62.65	18.78	18.84
13	20090210	20091229	1690.94	322	HH	HH	38.22	10.47	12.94
14	20090210	20100213	2226.04	368	HH	HH	29.00	12.46	13.03
15	20091229	20100213	553.26	46	HH	HH	115.98	30.87	21.88
16	20091229	20100331	719.75	92	HH	HH	88.78	8.92	8.57
17	20091229	20101001	1677.84	276	HH	HH/HV	38.26	43.45	33.66
18	20091229	20101116	1320.82	322	HH	HH	48.62	6.55	8.95
19	20100213	20101001	1124.73	230	HH	HH/HV	57.08	22.61	21.56
20	20100213	20101116	781.46	276	HH	HH	82.61	14.49	23.49
21	20100331	20101001	975.78	184	HH	HH/HV	65.83	16.30	14.71
22	20100331	20101116	673.44	230	HH	HH	96.42	9.16	12.89

Two fusion methods for the production of the mosaic DEM were applied. For the second method, an ancillary DEM is required during the mosaic production procedure. In this study, the ASTER GDEM v2 (released October 2011) has been used. It is a DEM with 30m grid spacing. Its vertical accuracy has been estimated to be 16.20m according to the GCPs, and 10.74m according to the reference DEM (rDEM).

The fusion methods have been applied on three groups of interferometric-based DEMs. The first group included the interferometric-based DEMs whose RMS errors were less than 10m, according to GCPs evaluation i.e. 3 DEMs. The second group included those DEMs with RMS errors less than 15m, i.e. 7 DEMs, and the third group included all the interferometric-based DEMs, i.e. 22 DEMs (Table 2). Moreover, for the second fusion method, various thresholds were tested in order to

optimize the value of the threshold that is required for masking the interferometric-based DEMs and height precision files.

Table 2. Range of RMS error for the three formed data groups.

	RMS Error (m)			
	According to GCPs		According to rDEM	
	min	max	min	max
1st Group (3 DEMs)	6.55	9.16	8.57	12.89
2nd Group (7 DEMs)	6.55	14.53	8.57	23.49
3rd Group (22 DEMs)	6.55	45.14	8.57	38.21

4. Results

Figure 2 shows the results of the validation of the fusion-based DEMs. In the horizontal axis, the numbers correspond to the following: (1) is for the 1st fusion Method and (2), (3), (4), (5) and (6) are for the 2nd fusion Method and for threshold value 5m, 10m, 20m, 30m and 40m, respectively. It is observed that both fusion methods do not achieve to improve the vertical accuracy of the mosaic DEM when all the raw interferometric-based DEMs are used (22 DEMs). The RMS error of the mosaic DEMs is always higher than 6.55m (Table 2) which is the least error produced by the individual interferometric pairs (Figure 2a). An improvement in accuracy is observed only when the 2nd fusion method is applied and the mosaic DEM is compared with the rDEM. The best RMS error in this case is approximately 8m and achieved when the threshold value is defined 20 (abscissa 4) or 30m (abscissa 5) (Figure 2b, green line). These threshold values confirm that it is necessary to define an upper limit on the RMS error for the areas presented in the interferometric-based DEMs, in order to mask them and optimize the fusion procedure. On the other hand, a very low threshold value, for example 5 meters, does not improve the accuracy. The more interferometric-based DEMs are used, the smaller the contribution of each DEM to the mosaic DEM is. The contribution of each DEM in the final mosaic DEM depends only on the pixel value in the respective height accuracy map file. Therefore, the contribution of each DEM, either positive or negative, is lower in case that more DEMs are involved in the production of the mosaic DEM.

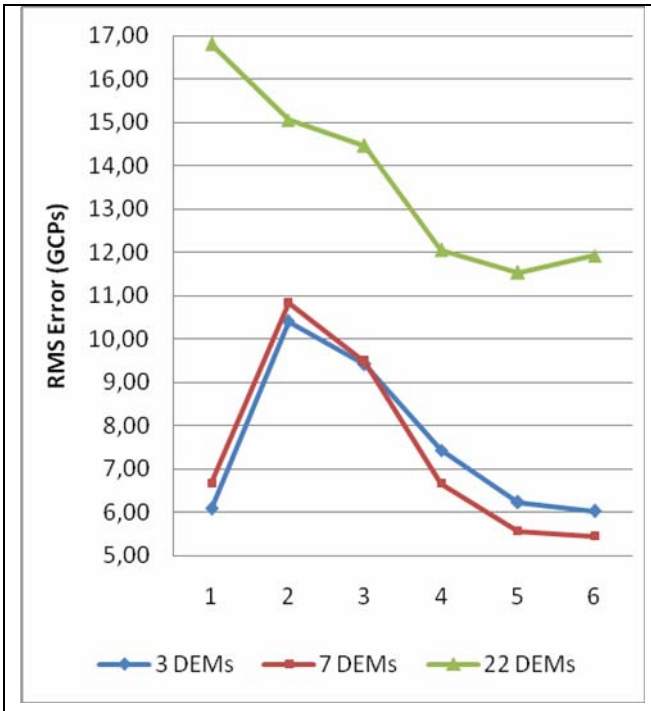

(a)

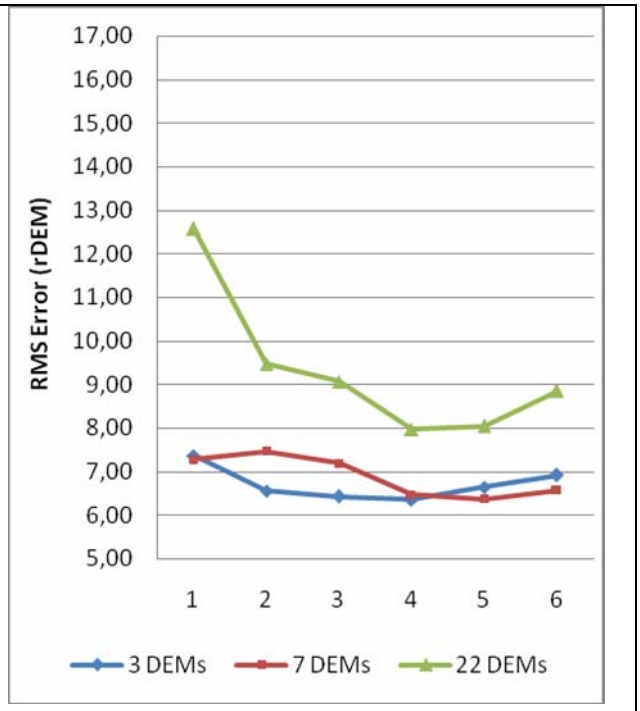

(b)

Figure 2: RMSE produced by the two fusion techniques (a) GCPs evaluation (b) rDEM evaluation. In x axis, abscissa (1) is for the 1st fusion Method and abscissas (2), (3), (4), (5) and (6) are for the 2nd fusion Method and for threshold value 5m, 10m, 20m, 30m and 40m, respectively.

The results are more encouraging when the involved DEMs in the mosaic methods are selected under specific evaluation criteria. For example, for the second group (7 DEMs, red line) by applying the 1st method, there is no improvement in the vertical accuracy of the mosaic DEM since RMS error is 6.68m according to the GCPs evaluation (Figure 2a), and it is almost similar to the minimum error, given in Table 2. However, an improvement in accuracy is observed according to the rDEM evaluation (7.28m), (Figure 2b). Consequently, an improvement of the accuracy of the elevation model is achieved, even if locally, in specific points, there is no improvement. The application of the 2nd method produces results which depend on the choice of the threshold. From Figures 2a and 2b it is observed that as the selected threshold approaches the vertical accuracy of the ancillary DEM for confidence level 95%, which is approximately 32m (=1.96*16.20), there is a significant improvement in the vertical accuracy of the mosaic DEM. Specifically for threshold 30m (abscissa 5, Fig 2a, 2b), RMS errors are 5.56m and 6.37m for GCPs and rDEM evaluation, respectively. Additionally, the RMS error produced by the GCPs evaluation is less for 50m threshold (Figure 2a), but by taking into account the evaluation with both techniques (Figure 2a, 2b), it is concluded that the optimal result is achieved for 30m threshold or otherwise for the vertical accuracy of the ancillary DEM. Comparing the two applied fusion methods it is concluded that the proposed method reduces the average RMS error about 1.1m based on the GCPs evaluation and about 0.9m based on the rDEM evaluation, respectively.

As far as the first group (3 DEMs, blue line) is concerned, only 30 and 40m thresholds (abscissas 5 and 6) were considered for the evaluation of the second method, since these thresholds have been proved to be optimal. Both fusion methods yielded an improvement in the vertical accuracy of the mosaic DEM which however is less than that produced by the second group. According to the GCPs evaluation, the two fusion methods produced almost similar errors in the range of 6m. However, rDEM evaluation showed that the proposed method produced higher errors

about 6.40m. Based on both evaluation techniques the threshold of 30m, i.e. the vertical accuracy of the ancillary DEM for confidence level 95%, is the optimum for the application of the proposed method on the specific data.

Comparing the validation results of the first and second group of data, it is concluded that the optimal vertical accuracy is not achieved on the mosaic DEM when using the interferometric-based DEMs with the best accuracy (group 1). On the contrary, the optimum result is achieved when a broader number of interferometric-based DEMs is used which meets specific accuracy criteria. Finally, it is noteworthy to point out that both methods generated only few or no void pixels in the final mosaic DEM. The first fusion method is almost independent from the number of the used DEMs (Figure 3). On the other hand, the second fusion method depends not only on the number of the interferometric-based DEMs which participated in the production of the mosaic DEM but also on the choice of the threshold (Figure 3). Moreover, from Figure 3 it is observed the higher the number of interferometric-based DEMs, the faster and smoother convergence is achieved regarding the optimal percentage of non void pixels, i.e.100%.

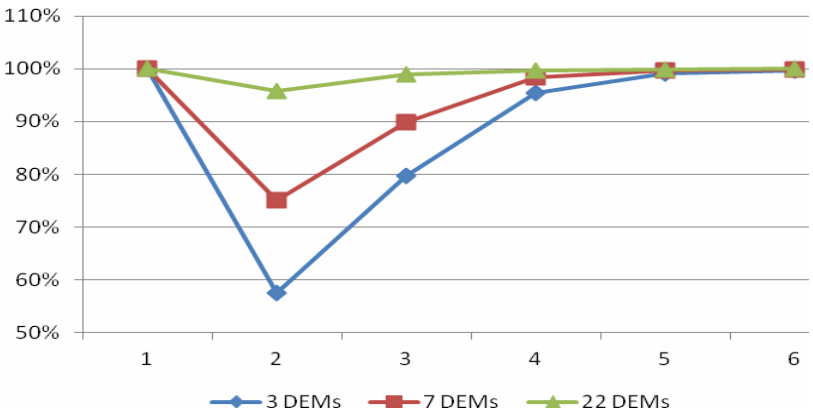

Figure 3: The percentage of non void pixels in the DEMs produced by the fusion methods.

5. Conclusions

Two fusion methods were applied and tested for the production of a mosaic DEM surface using interferometric-based DEMs. The first is a state of the art method whereas the second is an improvement of the first, proposed within this study. Both methods were based on the weighted average height. Weights were provided by the height accuracy map files, produced by the SARscape software. However, height accuracy maps are not always consistent with the accuracy of the interferometric-based DEMs. In the first method, the entire height information was used for each interferometric-based DEM, while in the second method only selected areas participated in the procedure. Area selection was made using an ancillary DEM. Experiments showed that the selected areas from each interferometric-based DEM should present accuracy higher than the vertical accuracy of the used ancillary DEM for confidence level 95%, in order to improve the final result.

The proposed approach improved the vertical accuracy of the produced mosaic DEM even in case that the used height accuracy maps were not reliable. The optimum result has been achieved when specific accuracy criteria, i.e. overall accuracy better than 15m, were set on the interferometric-based DEMs that participated into the fusion procedure. In this case, the method improved about 1m the vertical accuracy of the DEM, by producing the minimum RMS error (5.56m).

The study of geomorphological characteristics of the regions of the interferometric-based DEMs that present low accuracy, as well as the improvement of the quality of the height accuracy maps need further investigation and will be studied in future work.

Acknowledgements

The authors would like to acknowledge KTIMATOLOGIO S.A. for kindly providing the reference DEM for the study area. ALOS/PALSAR SAR acquisitions were provided by ESA-3728.

References

[1] Bamler, R., 1997. Digital Terrain Models from Radar Interferometry. In: *Photogrammetric Week 1997*, edited by D. Fritch & D. Hobbie (Wichmann Verlag, Heidelberg), pp. 93-105.

[2] Bamler, R. and Hartl, P., 1998. Synthetic aperture radar interferometry. *Inverse Problems*, 14 (4): R1-R54.

[3] Rosen, P. A., Hensley, S., Joughin, I. R., Li, F. K., Madsen, S. N., Rodríguez, E. and Goldstein, R. M., 2000. Synthetic Aperture Radar Interferometry. In: *Proceedings of the IEEE*, 88 (3): pp. 333-382.

[4] Roth, A., Knopfle, W., Strunz, G., Lehner, M. and Reinartz, P., 2002. Towards a global elevation product: combination of multi-source digital elevation models. In: *Joint International Symposium on Geospatial Theory, Processing and Applications.*

[5] Schindler, K., Papasaika-Hanusch, H., Schutz, S. and Baltsavias, E., 2011. *Improving Wide-Area DEMs Through Data Fusion – Chances and Limits*, ETH Publications.

[6] Papasaika, H., Poli, D. and Baltsavias, E., 2008. A framework for the fusion of Digital Elevation Models. In: *Proceedings of the XXI ISPRS Congress*, Beijing, China, pp. 811-817.

[7] Papasaika, H. and Baltsavias, E., 2009. Fusion of LiDAR and Photogrammetric Generated Digital Elevation Models. In: *Proceedings of the ISPRS Hannover Workshop on High-Resolution Earth Imaging for Geospatial Information*, Hannover, Germany.

[8] Papasaika, H., Kokiopoulou, E., Baltsavias, E., Schindler, K. and Kressner, D., 2011. Fusion of Digital Elevation Models Using Sparse Representations. In: *Proceedings of the Photogrammetric Image Analysis*, Munich, Germany.

[9] Schultz, H., Riseman, E. M., Stolle, F. R. and Woo, D. M., 1999. Error detection and DEM fusion using self-consistency. In: *International Conference on Computer Vision*.

[10] Honikel, M., 1999. Strategies and methods for the fusion of digital elevation models from optical and SAR data. In: *International Archives of Photogrammetry and Remote Sensing*, 32(7-4-3W6), pp. 83–89.

[11] Damron, J., 2002. Fusing Lidar and IFSAR DEMs: a seven-step methodology. In: *22nd ESRI International Conference*.

[12] Gamba, P., Dell'Acqua, F. and Houshmand, B., 2003. Comparison and fusion of Lidar and InSAR digital elevation models over urban areas. *International Journal of Remote Sensing*, 24(22), pp. 4289–4300.

[13] Podobnikar, T., 2006. DEM from various data sources and geomorphic details enhancement. In: *5th ICA Mountain Cartography Workshop*.

[14] Knöpfle, W., Strunz, G. and Roth, A., 1998. Mosaicking of digital elevation models derived by SAR interferometry. In: Proceedings of the IAPRS, *ISPRS Commission IV Symposium on GIS-Between Visions and Applications*, 32 (4): pp. 306-313.

[15] Costantini, M., Malvarosa, F., Minati, F. and Zappitelli, E., 2006. A Data Fusion Algorithm for DEM Mosaicking: Building a Global DEM with SRTM-X and ERS Data. In: *Proccedings of the Geo, science and Remote Sensing Symposium*, 2006. IGARSS 2006. pp. 3844-3847.

[16] Gens, R. and Van Genderen, J. L., 1996. SAR interferometry-issues, techniques, applications. *International Journal of Remote Sensing*, 17(10): pp. 1803-1835.

[17] SARscape, http://www.sarmap.ch.

[18] Chousiafis, C., 2011. Development of a mosaic methodology for the optimal production of Digital Elevation Model using repeat pass interferometry, Diploma Thesis, NTUA, Greece (in Greek).

[19] Zhou, C., Ge L., E D. and Chang H. C., 2005. A case study of using external DEM in InSAR DEM generation. *GeoSpatial Information Science*, 8(1): pp. 14-18.

[20] Yu, G.-H. and Ge L., 2010. Digital Elevation Model generation using ascending and descending multi-baseline ALOS/PALSAR radar images. In: *FIG Congress 2010*.